JACS
JOURNAL OF THE AMERICAN CHEMICAL SOCIETY

Communication

pubs.acs.org/JACS

Step-by-Step Fabrication of a Highly Oriented Crystalline Three-Dimensional Pillared-Layer-Type Metal–Organic Framework Thin Film Confirmed by Synchrotron X-ray Diffraction

Kazuya Otsubo,*[,†,‡] Tomoyuki Haraguchi,[†] Osami Sakata,[‡,§] Akihiko Fujiwara,[‡,∥] and Hiroshi Kitagawa*[,†,‡,⊥,▽]

[†]Division of Chemistry, Graduate School of Science, Kyoto University, Kitashirakawa Oiwake-cho, Sakyo-ku, Kyoto 606-8502, Japan

[‡]Core Research for Evolutional Science and Technology (CREST), Japan Science and Technology Agency (JST), 5 Sanban-cho, Chiyoda-ku, Tokyo 102-0075, Japan

[§]Synchrotron X-ray Station at SPring-8, National Institute for Materials Science (NIMS), 1-1-1 Kouto, Sayo-cho, Sayo-gun, Hyogo 679-5148, Japan

[∥]Japan Synchrotron Radiation Research Institute (JASRI), SPring-8, 1-1-1 Kouto, Sayo-cho, Sayo-gun, Hyogo 679-5198, Japan

[⊥]Institute for Integrated Cell-Material Sciences (iCeMS), Kyoto University, Yoshida, Sakyo-ku, Kyoto 606-8501, Japan

[▽]INAMORI Frontier Research Center, Kyushu University, 744 Motooka, Nishi-ku, Fukuoka 819-3095, Japan

Supporting Information

ABSTRACT: Fabrication of a crystalline ordered thin film based on the porous metal–organic frameworks (MOFs) is one of the practical applications of the future functional nanomaterials. Here, we report the creation of a highly oriented three-dimensional (3-D) porous pillared-layer-type MOF thin film on a metal substrate using a step-by-step approach based on liquid-phase epitaxy. Synchrotron X-ray diffraction (XRD) study clearly indicates that the thin film is crystalline and its orientation is highly controlled in both horizontal and vertical directions relative to the substrate. This report provides the first confirmation of details of not only the crystallinity but also the orientation of 3-D MOF thin film using synchrotron XRD. Moreover, we also demonstrate its guest adsorption/desorption behavior by using *in situ* XRD measurements. The results presented here would promise useful insights for fabrication of MOF-based nanodevices in the future.

Recent progress in porous metal–organic frameworks (MOFs),[1] which are crystalline polymeric materials composed of metal ions and multidentate organic ligands, has yielded a wide range of rich science, such as gas-sorption,[2] catalytic,[3] conducting,[4] magnetic,[5] and electronic[6] properties derived from their large porosity and designability of structures. In light of their availability, efficient use of pore space, and integrating functions, fabrication of porous MOFs as a thin film is one of the challenges for the development of future important nanomaterials such as electronic, catalytic, and sensing devices. Therefore, development of MOF thin films on a solid surface has recently attracted significant attention.[7]

For application use of MOF thin films, controlling their crystalline orientation, which is confirmed mainly using X-ray diffraction (XRD) along both horizontal and vertical directions (i.e., in-plane and out-of-plane directions) relative to the substrate surface, is essential. Although there have been many attempts to date, in general, it is difficult to fabricate highly oriented crystalline MOF thin films because many of them are polycrystalline where their growth directions can be hardly controlled.[8] Moreover, even if they are obtained, their low thickness and density values cause difficulties in structural characterization using XRD measurements. To control not only the number of layers but also the growth directions of MOF thin films, two approaches have been intensively studied. One is a step-by-step approach in the liquid phase using a solution of structural components and functionalized substrates, such as a self-assembled monolayer (SAM) on Au.[9] The other is a novel film fabrication approach that is a combination of the Langmuir–Blodgett and layer-by-layer methods (LB–LbL).[10] By using this LB–LbL method, we have recently achieved construction of highly oriented crystalline porphyrin-based two-dimensional (2-D) layered MOF thin films. In addition, these techniques also allow thin-film growth to be monitored by optical techniques. In contrast to the development of MOF thin-film preparation, structural confirmation including their crystalline orientation is still a major puzzle that should be noted. Most crystalline MOF thin films whose orientation could be perfectly controlled along both in-plane and out-of-plane directions to the substrate are mainly limited to 2-D layer-type MOFs.[9d,10] Although there are several crystalline 3-D network-type MOF thin films,[9a−c,e,f] many of them have been structurally confirmed only by out-of-plane XRD measurements, and there are only a few examples with perfectly controlled orientation confirmed by both in-plane and out-of-plane XRD measurements.[9f]

Here, we show the fabrication and structural confirmation of a highly oriented crystalline 3-D porous pillared-layer-type MOF thin film. By using synchrotron surface XRD measurements, we demonstrate that the crystalline orientation of this

Received: May 5, 2012
Published: May 31, 2012

dx.doi.org/10.1021/ja304361v | J. Am. Chem. Soc. 2012, 134, 9605–9608

film is perfectly controlled along both in-plane and out-of-plane directions relative to the substrate. In this work, we focused on a Hofmann-type clathrate MOF, $Fe(pz)[Pt(CN)_4]$ (pz: pyrazine) as a target material to fabricate the thin film on the substrate because it has a simple porous 3-D network with a pillared-layer structure where the cyanide-bridged 2-D layers containing Fe and $Pt(CN)_4$ units are connected to each other by a pz ligand to form a 3-D lattice. Hofmann-type clathrate MOFs have been intensively studied because of their magnetic properties (e.g., spin-crossover behavior) which are thermally or optically induced, and sorption properties for many guest molecules.[11] Deposition of $Fe(pz)[Pt(CN)_4]$ on a metal substrate has been reported previously;[12] however, confirmation of its crystallinity and orientation based on the X-ray study has not been achieved yet. In general, in the case of such Hofmann-type MOFs, it is difficult to obtain the single crystals even in bulk syntheses because of their poor crystallinity similar to cyanide-bridged Prussian blue analogues. Therefore, the thin films composed of Hofmann-type MOFs have not been considered as crystalline and oriented thin films to date.[7] Because the use of Hofmann-type MOFs as thin film is surely an attractive research target for future optical and electronic devices, clarification of the structural aspects is one of the imperative tasks that would contribute to practical applications. In our work, we used a Au/Cr/Si substrate by which a highly oriented crystalline MOF thin film was fabricated using the LbL method,[10b] and a modified film preparation where we did not use an anchoring layer of 4,4′-azopyridine on the thiol-based SAM. Synchrotron XRD measurements on this $Fe(pz)[Pt(CN)_4]$ thin film show clear evidence not only for the crystallinity but also for the high orientation. In addition, we also demonstrate the guest adsorption/desorption behavior of this film by using XRD.

Preparation of the thin film was performed as follows (Figure 1).[13] First, the Au/Cr/Si substrate was soaked in an ethanol (EtOH) solution of 4-mercaptopyridine for a day to be functionalized by thiol-based SAM. After this treatment, the substrate was washed with EtOH and dried by N_2 flow. Next, this substrate was alternately soaked in EtOH solutions of $Fe(BF_4)_2{\cdot}6H_2O$, $[(C_4H_9)_4N]_2Pt(CN)_4$, and pz in this order at 212 K for a total of 30 cycles. In these soakings after the preparation of the SAM functionalized substrate, the 2-D layer structure containing Fe and $Pt(CN)_4$, and pillars of pz were alternately introduced into the substrate (see Figure 1). The substrate was washed with EtOH after each soaking.

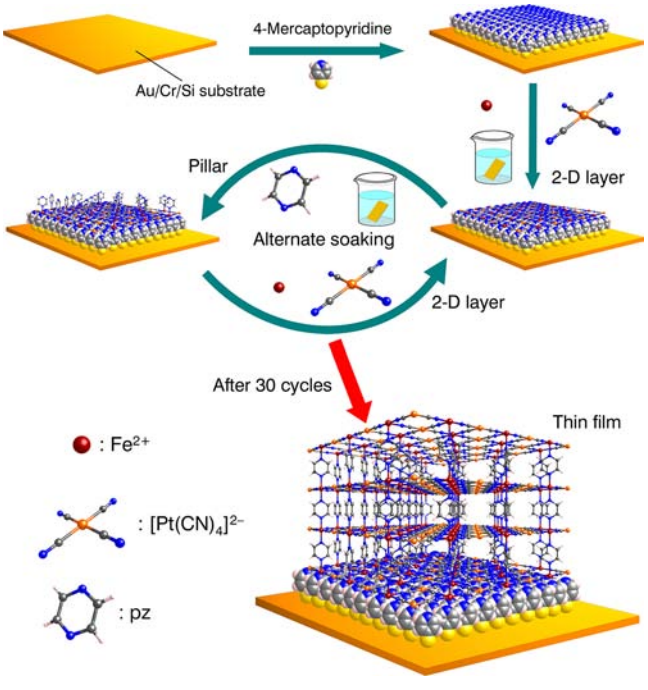

Figure 1. Schematic representation of the step-by-step approach to fabricating $Fe(pz)[Pt(CN)_4]$ thin film in the liquid phase.

The $Fe(pz)[Pt(CN)_4]$ thin-film growth could be monitored using infrared reflection absorption spectroscopy (IRRAS). Figure 2 shows the IRRAS of the $Fe(pz)[Pt(CN)_4]$ thin film for each synthetic cycle. The peak intensity of the ν(CN) stretching mode derived from the 2-D layer around 2170 cm^{-1} clearly increased with an increase in the number of cycles as was expected. In addition, as shown in the inset of Figure 2, there was a linear increase in maximum absorbance with increasing number of cycles, indicating successive growth of the film. We also recorded the Raman spectrum on the obtained film. As shown in Supporting Information, Figure S1, the Raman spectrum agreed well with the bulk sample of $Fe(pz)[Pt(CN)_4]$ in the high-spin (HS) state.

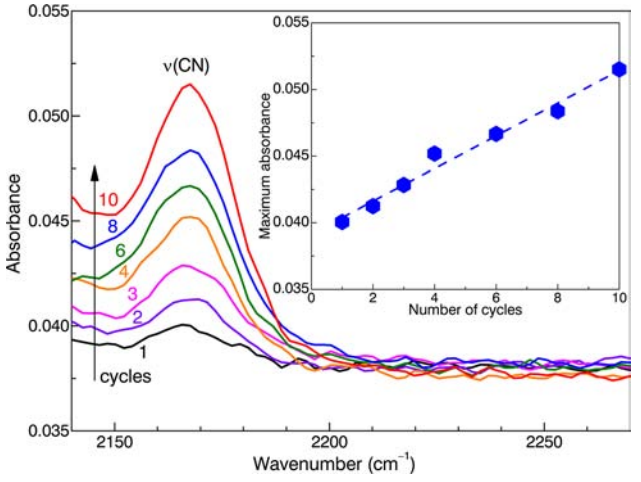

Figure 2. Step-by-step thin-film growth monitored by IRRAS at rt. (Inset) Dependence of the maximum absorbance of the ν(CN) mode on the number of cycles. The blue dotted line is a visual guide.

As described above, it is generally difficult to confirm the crystal structure and orientation of MOF thin films using an XRD measurement because of the low thickness and density of the films. In such a case, using synchrotron radiation is a powerful technique that offers high-quality structural information because of the high photon flux density. To investigate its crystallinity and orientation on the substrate of the obtained thin film, synchrotron surface XRD measurements were carried out at the BL13XU beamline of SPring-8.[14] Figure 3 shows synchrotron XRD patterns (λ = 1.555 Å, room temperature (rt)) of the 30-layer film both in the horizontal direction (in-plane, grazing-incidence mode; Figure 3a) and in the vertical direction (out-of-plane, θ–2θ mode; Figure 3b) relative to the substrate. By comparing these with simulated XRD patterns (denoted as green lines in Figure 3) obtained from bulk $Fe(pz)[Pt(CN)_4]$, we successfully proved the highly oriented nature of this thin film. As shown in Figure 3a, several peaks that can be indexed as 100, 110, 200, 210, 220, 300, and 310

dx.doi.org/10.1021/ja304361v | J. Am. Chem. Soc. 2012, 134, 9605–9608

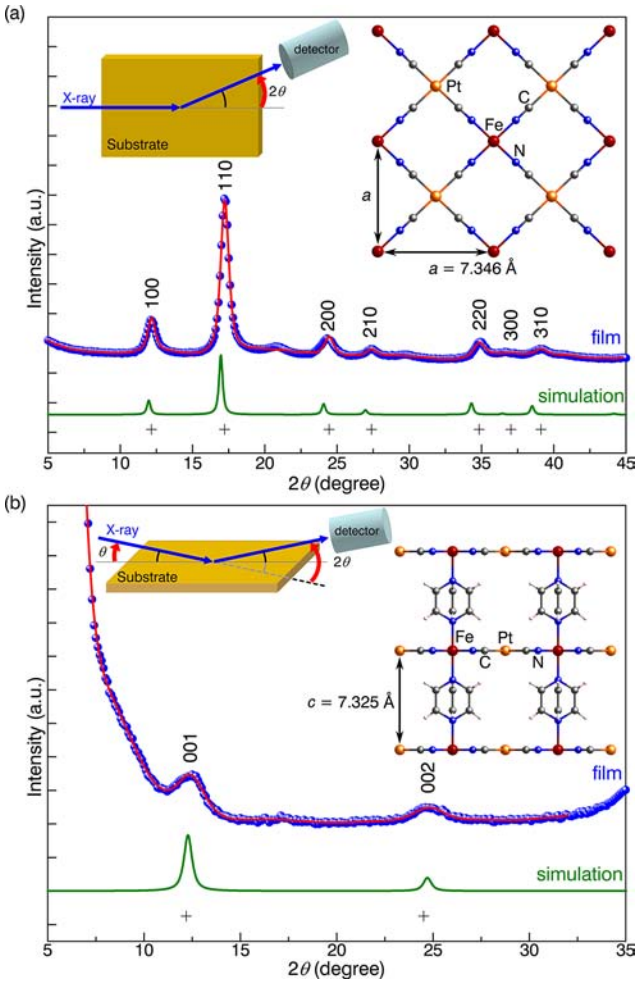

Figure 3. Synchrotron XRD patterns of $Fe(pz)[Pt(CN)_4]$ thin film (λ = 1.555 Å, rt). (a) In-plane XRD pattern. (b) Out-of-plane XRD pattern. Blue circles, red lines, green lines, and black crosses in each panel denote experimental data, fitting results, simulated diffraction patterns, and observed Bragg peaks, respectively. Inset figures in each panel denote the scattering geometries of the XRD study and periodic orderings observed in each diffraction pattern. The gradual increase in the background above 30° in Figure 3b is derived from strong diffraction by Au.

were observed in the in-plane diffraction. By contrast, the out-of-plane diffraction pattern (Figure 3b) revealed the existence of two diffraction peaks that can be indexed as 001 and 002. It should be noted that *hk*0 and 00*l* diffraction peaks are separately observed in the in-plane and out-of-plane XRD measurements, respectively. Therefore, the in-plane XRD pattern shows a periodic ordering of the cyanide-bridged 2-D layer, and the out-of-plane diffraction pattern corresponds to the pz ligand-mediated interlayer spacing, as shown in the insets of Figure 3. The synchrotron XRD technique provides clear evidence that the obtained thin film is highly crystalline and its orientation is perfectly controlled. The obtained in-plane and out-of-plane XRD patterns lead its tetragonal lattice with a = 7.346 Å and c = 7.325 Å, values that are in good agreement with the values of the bulk sample in the HS state (tetragonal, $P4/mmm$, a = 7.457 Å and c = 7.259 Å, data from ref 11b). To obtain further structural information on this film, we also carried out rocking curve (θ-scan mode) and azimuthal-angle dependence (ϕ-scan mode) measurements at the 001 position (Supporting Information, Figure S2). The rocking curve shows a weak single peak around 6.2° with full-width at half-maximum (fwhm) of 3.4°, suggesting that each 2-D layer is stacked with an average tilting angle of ~3.4°. Hence, the absence of azimuthal angle dependence within the surface of the substrate clearly indicates that the obtained film is uniformly fabricated with no preference in the substrate. The crystalline domain size of this film estimated from fwhm of intense 110 diffraction peak using Scherrer's equation was ca. 14 nm. Several domains could be observed in the atomic force microscopy (AFM) image of this film (Supporting Information, Figure S3). Some large domains had a side of 50−100 nm, while other small domains had a side of <20 nm. Therefore, because of the large size dispersion of the domains as seen in the AFM image, the crystalline domain size would be estimated as a small value in the X-ray observation.

Because the bulk material of $Fe(pz)[Pt(CN)_4]$ exhibits adsorption properties for several guest molecules such as H_2O, EtOH, benzene (bz), H_2, and CO_2, among others, we also investigated the guest adsorption/desorption behavior of the thin film. In this study, bz was selected as the probe because it has a larger molecular size than the other guest species. Figure 4

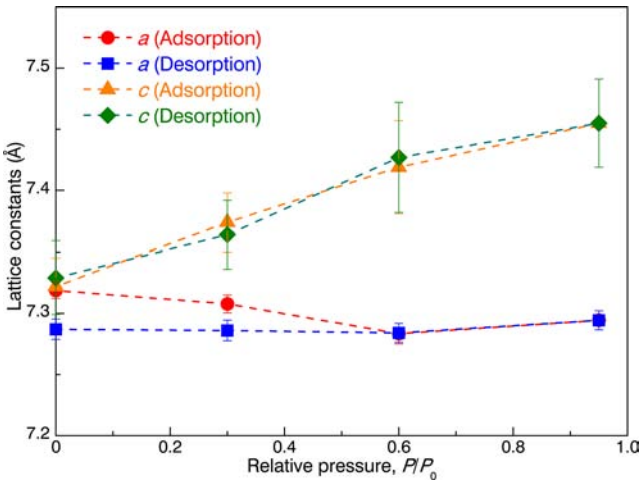

Figure 4. Benzene adsorption/desorption behavior detected from changes in the lattice constants, a (obtained from in-plane XRD) and c (obtained from out-of-plane XRD) at rt. P/P_0 denotes relative pressure, where P_0 is saturated vapor pressure of benzene at rt (13.44 kPa).

shows changes in the lattice constants (a and c) of the obtained thin film calculated from in situ XRD measurements under several vapor pressures of bz at rt. As clearly seen in Figure 4, no significant change in lattice constant a, which corresponds to the intralayer spacing, was observed with varying bz vapor pressure. However, a reversible increase/decrease of interlayer spacing (i.e., lattice constant c) was observed, implying that reversible bz adsorption/desorption occurred in the thin film.

In summary, we have described the successful fabrication and structural confirmation of a highly oriented crystalline Hofmann-type porous 3-D MOF, $Fe(pz)[Pt(CN)_4]$ thin film. By using high quality synchrotron surface XRD results, we clearly demonstrated that this film is crystalline, and its orientation is perfectly controlled. Preparations, structural determinations, and investigations of gas-sorption properties of metal-ion exchanged MOF thin films and heterostructured thin films are now in progress.

dx.doi.org/10.1021/ja304361v | J. Am. Chem. Soc. 2012, 134, 9605−9608

■ ASSOCIATED CONTENT

Supporting Information

Details of experimental procedure, thin film preparation, Raman spectrum, additional XRD data, and AFM image. This material is available free of charge via the Internet at http://pubs.acs.org.

■ AUTHOR INFORMATION

Corresponding Author

kazuya@kuchem.kyoto-u.ac.jp; kitagawa@kuchem.kyoto-u.ac.jp

Notes

The authors declare no competing financial interests.

■ ACKNOWLEDGMENTS

Synchrotron XRD measurements were supported by the Japan Synchrotron Radiation Research Institute (JASRI) (Proposal No. 2010B1535, No. 2011A1463 and No. 2011B1013). This work was partly supported by the Grants-in-Aid for Scientific Research No. 20350030 and No. 23245012 by the Ministry of Education, Culture, Sports, Science and Technology of Japan.

■ REFERENCES

(1) (a) Yaghi, O. M.; O'Keeffe, M.; Ockwig, N. W.; Chae, H. K.; Eddaoudi, M.; Kim, J. *Nature* **2003**, *423*, 705. (b) Kitagawa, S.; Kitaura, R.; Noro, S. *Angew. Chem., Int. Ed.* **2004**, *43*, 2334. (c) Ferey, G. *Chem. Soc. Rev.* **2008**, *37*, 191.

(2) (a) Chae, H. K.; Siberio-Perez, D. Y.; Kim, J.; Go, Y.; Eddaoudi, M.; Matzger, A. J.; O'Keeffe, M.; Yaghi, O. M. *Nature* **2004**, *427*, 523. (b) Ferey, G.; Mellot-Draznieks, C.; Serre, C.; Millange, F.; Dutour, J.; Surble, S.; Margiolaki, I. *Science* **2005**, *309*, 2040. (c) Murray, L. J.; Dinca, M.; Long, J. R. *Chem. Soc. Rev.* **2009**, *38*, 1294. (d) Shimomura, S.; Higuchi, M.; Matsuda, R.; Yoneda, K.; Hijikata, Y.; Kubota, Y.; Mita, Y.; Kim, J.; Takata, M.; Kitagawa, S. *Nat. Chem.* **2010**, *2*, 633. (e) Li, J. R.; Sculley, J.; Zhou, H. C. *Chem. Rev.* **2012**, *112*, 869. (f) Sumida, K.; Rogow, D. L.; Mason, J. A.; McDonald, T. M.; Bloch, E. D.; Herm, Z. R.; Bae, T. H.; Long, J. R. *Chem. Rev.* **2012**, *112*, 724. (g) Kreno, L. E.; Leong, K.; Farha, O. K.; Allendorf, M.; Van Duyne, R. P.; Hupp, J. T. *Chem. Rev.* **2012**, *112*, 1105.

(3) (a) Seo, J. S.; Whang, D.; Lee, H.; Jun, S. I.; Oh, J.; Jeon, Y. J.; Kim, K. *Nature* **2000**, *404*, 982. (b) Wu, C. D.; Hu, A.; Zhang, L.; Lin, W. *J. Am. Chem. Soc.* **2005**, *127*, 8940. (c) Wu, C. D.; Lin, W. *Angew. Chem., Int. Ed.* **2007**, *46*, 1075. (d) Farha, O. K.; Shultz, A. M.; Sarjeant, A. A.; Nguyen, A. T.; Hupp, J. T. *J. Am. Chem. Soc.* **2011**, *133*, 5652. (e) Yoon, M.; Srirambalaji, R.; Kim., K. *Chem. Rev.* **2012**, *112*, 1196.

(4) (a) Kitagawa, H.; Onodera, N.; Sonoyama, T.; Yamamoto, M.; Fukuwa, T.; Mitani, T.; Seto, M.; Maeda, Y. *J. Am. Chem. Soc.* **1999**, *121*, 10068. (b) Fuma, Y.; Ebihara, M.; Kutsumizu, S.; Kawamura, T. *J. Am. Chem. Soc.* **2004**, *126*, 12238. (c) Otsubo, K.; Kobayashi, A.; Kitagawa, H.; Hedo, M.; Uwatoko, Y.; Sagayama, H.; Wakabayashi, Y.; Sawa, H. *J. Am. Chem. Soc.* **2006**, *128*, 8140. (d) Sadakiyo, M.; Yamada, T.; Kitagawa, H. *J. Am. Chem. Soc.* **2009**, *131*, 9906. (e) Bureekaew, S.; Horike, S.; Higuchi, M.; Mizuno, M.; Kawamura, T.; Tanaka, D.; Yanai, N.; Kitagawa, S. *Nat. Mater.* **2009**, *8*, 831. (f) Hurd, J. A.; Vaidhyanathan, R.; Thangadurai, V.; Ratcliffe, C. I.; Moudrakovski, I. L.; Shimizu, G. K. H. *Nat. Chem.* **2009**, *1*, 705. (g) Givaja, G.; Amo-Ochoa, P.; Gómez-García, C. J.; Zamora, F. *Chem. Soc. Rev.* **2012**, *41*, 115. (h) Jeong, N. C.; Samanta, B.; Lee, C. Y.; Farha, O. K.; Hupp, J. T. *J. Am. Chem. Soc.* **2012**, *134*, 51. (i) Sadakiyo, M.; Ōkawa, H.; Shigematsu, A.; Ohba, M.; Yamada, T.; Kitagawa, H. *J. Am. Chem. Soc.* **2012**, *134*, 5472.

(5) (a) Tamaki, H.; Zhong, Z. J.; Matsumoto, N.; Kida, S.; Koikawa, M.; Achiwa, N.; Hashimoto, Y.; Ōkawa, H. *J. Am. Chem. Soc.* **1992**, *114*, 6974. (b) Ohba, M.; Ōkawa, H. *Coord. Chem. Rev.* **2000**, *198*, 313. (c) Kaneko, W.; Ohba, M.; Kitagawa, S. *J. Am. Chem. Soc.* **2007**, *129*, 13706. (d) Ōkawa, H.; Shigematsu, A.; Sadakiyo, M.; Miyagawa, T.; Yoneda, K.; Ohba, M.; Kitagawa, H. *J. Am. Chem. Soc.* **2009**, *131*, 13516. (e) Kurmoo, M. *Chem. Soc. Rev.* **2009**, *38*, 1353.

(6) (a) Kitaura, R.; Fujimoto, K.; Noro, S.; Kondo, M.; Kitagawa, S. *Angew. Chem., Int. Ed.* **2002**, *41*, 133. (b) Ohmori, O.; Kawano, M.; Fujita, M. *J. Am. Chem. Soc.* **2004**, *126*, 16292. (c) Shimomura, S.; Horike, S.; Matsuda, R.; Kitagawa, S. *J. Am. Chem. Soc.* **2007**, *129*, 10990. (d) Otsubo, K.; Wakabayashi, Y.; Ohara, J.; Yamamoto, S.; Matsuzaki, H.; Okamoto, H.; Nitta, K.; Uruga, T.; Kitagawa, H. *Nat. Mater.* **2011**, *10*, 291. (e) Martí-Rujas, J.; Islam, N.; Hashizume, D.; Izumi, F.; Fujita, M.; Song, H. J.; Choi, H. C.; Kawano, M. *Angew. Chem., Int. Ed.* **2011**, *50*, 6105.

(7) For reviews of recent developments in MOF thin films, see (a) Shekhah, O.; Liu, J.; Fischer, R. A.; Wöll, C. *Chem. Soc. Rev.* **2011**, *40*, 1081. (b) Zacher, D.; Schmid, R.; Wöll, C.; Fischer, R. A. *Angew. Chem., Int. Ed.* **2011**, *50*, 176. (c) Bétard, A.; Fischer, R. A. *Chem. Rev.* **2012**, *112*, 1055.

(8) (a) Zacher, D.; Baunemann, A.; Hermes, S.; Fischer, R. A. *J. Mater. Chem.* **2007**, *17*, 2785. (b) Gascon, J.; Aguado, S.; Kapteijn, F. *Microporous Mesoporous Mater.* **2008**, *113*, 132. (c) Hermes, S.; Schröder, F.; Chelmowski, R.; Wöll, C.; Fischer, R. A. *J. Am. Chem. Soc.* **2005**, *127*, 13744. (d) Yoo, Y.; Jeong, H. K. *Cryst. Growth Des.* **2010**, *10*, 1283.

(9) (a) Shekhah, O.; Wang, H.; Kowarik, S.; Schreiber, F.; Paulus, M.; Tolan, M.; Sternemann, C.; Evers, F.; Zacher, D.; Fischer, R. A.; Wöll, C. *J. Am. Chem. Soc.* **2007**, *129*, 15118. (b) Munuera, C.; Shekhah, O.; Wang, H.; Wöll, C.; Ocal, C. *Phys. Chem. Chem. Phys.* **2008**, *10*, 7257. (c) Shekhah, O.; Wang, H.; Paradinas, M.; Ocal, C.; Schüpbach, B.; Terfort, A.; Zacher, D.; Fischer, R. A.; Wöll, C. *Nat. Mater.* **2009**, *8*, 481. (d) Arslan, H. K.; Shekhah, O.; Wieland, D. C. F.; Paulus, M.; Sternemann, C.; Schroer, M. A.; Tiemeyer, S.; Tolan, M.; Fischer, R. A.; Wöll, C. *J. Am. Chem. Soc.* **2011**, *133*, 8158. (e) Hinterholzinger, F.; Scherb, C.; Ahnfeldt, T.; Stock, N.; Bein, T. *Phys. Chem. Chem. Phys.* **2010**, *12*, 4514. (f) Liu, B.; Shekhah, O.; Arslan, H. K.; Liu, J.; Wöll, C.; Fischer, R. A. *Angew. Chem., Int. Ed.* **2012**, *51*, 807.

(10) (a) Makiura, R.; Motoyama, S.; Umemura, Y.; Yamanaka, H.; Sakata, O.; Kitagawa, H. *Nat. Mater.* **2010**, *10*, 565. (b) Motoyama, S.; Makiura, R.; Sakata, O.; Kitagawa, H. *J. Am. Chem. Soc.* **2011**, *133*, 5640.

(11) (a) Niel, V.; Martínez-Agudo, J. M.; Muñoz, M. C.; Gaspar, A. B.; Real, J. A. *Inorg. Chem.* **2001**, *40*, 3838. (b) Ohba, M.; Yoneda, K.; Agustí, G.; Muñoz, M. C.; Gaspar, A. B.; Real, J. A.; Yamasaki, M.; Ando, H.; Nakao, Y.; Sakaki, S.; Kitagawa, S. *Angew. Chem., Int. Ed.* **2009**, *48*, 4767. (c) Agustí, G.; Ohtani, R.; Yoneda, K.; Gaspar, A. B.; Ohba, M.; Sánchez-Royo, J. F.; Muñoz, M. C.; Kitagawa, S.; Real, J. A. *Angew. Chem., Int. Ed.* **2009**, *48*, 8944.

(12) (a) Cobo, S.; Molnár, G.; Real, J. A.; Bousseksou, A. *Angew. Chem., Int. Ed.* **2006**, *45*, 5786. (b) Molnár, G.; Cobo, S.; Real, J. A.; Carcenac, F.; Daran, E.; Vieu, C.; Bousseksou, A. *Adv. Mater.* **2007**, *19*, 2163.

(13) See Supporting Information.

(14) Sakata, O.; et al. *Surf. Rev. Lett.* **2003**, *10*, 543.